

Properties and Stabilities of MX, MX₂, and M₂X₂ Compounds (M = Zn, Cd, Hg; X = F, Cl, Br, I)

Meng-sheng Liao and Qian-er Zhang

Chemistry Department, Xiamen University, Xiamen, Fujian, 361005, People's Republic of China

W. H. Eugen Schwarz*

Theoretische Chemie, Universität, D-57068 Siegen, Germany

Received May 3, 1995[⊗]

Free molecules MX, MX₂, M₂X₂, and M₂X₂(s) in the solid state (M = Zn, Cd, Hg; X = F, Cl, Br, I) are studied by using the relativistic density-functional method. The crystalline environment has been simulated by a cut-off type Madelung potential of point charges at the lattice sites. Energies, geometries, force constants, vibrational frequencies, and dipole moments have been determined. The calculated *molecular* properties are either in good agreement with available experimental data, they suggest their reinterpretation, or they are approximate predictions of so far unknown values. All M₂X₂ molecules, especially the Zn₂X₂ ones, are predicted to be stable against disproportionation in the gas phase, but the equilibrium is shifted toward MX₂ (especially for M = Zn and Cd) by condensation of the metal. The ligands and the crystal field are found to have a significant influence on the properties of the compounds. The calculated enthalpies of *solid* M₂X₂(s) reveal that they are unstable against decomposition into MX₂(s) + M(s) for M = Zn and Cd. The conclusions concerning the influence of differential aggregation energies drawn by Kaupp and von Schnering from pseudopotential calculations of the fluorides and chlorides are corroborated and extended. Relativity influences the energies and properties of Cd and especially of Hg compounds significantly in a complex manner, due to relativity–ionicity–cross effects.

1. Introduction

Mercury easily forms stable diatomic Hg₂²⁺ groups in solution and in the solid state, while Zn and Cd show a much smaller tendency towards dimerization.^{1,2} On the other hand, no *free* Hg₂²⁺, Zn₂²⁺, and Cd₂²⁺ ions have ever been observed experimentally. Theoretical studies show that free Hg₂²⁺ is at most metastable, and its bond energy is only very weakly influenced by relativity.^{3–5} This is in contrast to the isoelectronic free Au₂ molecule, which has a strong bond ($E_{\text{bond}}^{\text{exp}} = 2.3$ eV⁶) and which is remarkably stabilized by relativity ($\Delta^{\text{rel}}E_{\text{bond}} = 1.1$ eV^{7,8}). This paradoxon is due to a relativity–ionic repulsion cross term in the theoretical expression for the bond energy.^{3,5} It is apparent that the properties of free Hg₂²⁺ cannot explain the experimental evidence of Hg₂²⁺ in compounds.

In our previous works,^{4,9,10} we have performed a systematic investigation on free Hg₂²⁺, free Hg₂X₂ (X = F, Cl, Br, I) and

Hg₂X₂ in the crystals. The internal Hg–Hg bond energy as defined by the *dissociation* reaction



was shown to be notably *stabilized* by relativity, by the presence of electronegative ligands, and also by the crystal field. For the free Hg₂X₂ molecules, we obtained Hg–Hg bond energies of 2.2–2.8 eV, which are much larger than the corresponding bond energy in the metal (0.6 eV per Hg atom).

Since the radicals MX will disproportionate to MX₂ + M in the gas phase, the stabilities of M₂X₂ were also discussed with respect to the reaction



Various theoretical results^{4,9–11} indicate that the free Hg₂X₂ molecules are only slightly stable with respect to *disproportionation*, and relativity was found to *destabilize* the Hg₂X₂ system. Simple explanations of the exceptional stability of solid Hg(I) compounds as due to relativistic effects are therefore not acceptable. Consequently, it is still reasonable to ask why Zn₂X₂ and Cd₂X₂ do not exist and what are the causes affecting the stability of these compounds.

Using the quasi-relativistic pseudopotential, MP2, and CI Hartree–Fock methods, Kaupp and von Schnering¹¹ have recently investigated the special stability of Hg₂X₂ in the

* Author to whom correspondence should be addressed.

[⊗] Abstract published in *Advance ACS Abstracts*, October 1, 1995.

- (1) Aylett, B. J. In *Comprehensive Inorganic Chemistry*; Bailar, B. J., Emeléus, H. J., Trotman-Dickinson, A., Eds.; Pergamon Press: New York, 1973; Vol. 3.
- (2) Taylor, M. J. *Metal to Metal Bonded States of the Main Group Elements*, Academic Press: London, 1975.
- (3) Strömberg, D.; Wahlgren, U. *Chem. Phys. Lett.* **1990**, *169*, 109.
- (4) Liao, M. S. Ph.D. Thesis, Siegen University. Verlag Shaker: Aachen, Germany, 1993.
- (5) Schwarz, W. H. E.; Rutkowski, A.; Wang, S. G. *Int. J. Quantum Chem.*, in press.
- (6) (a) Huber, K. P.; Herzberg, G. *Molecular Spectra and Molecular Structure, Vol. IV, Constants of Diatomic Molecules*; Van Nostrand Reinhold: New York, 1979. (b) Givan A.; Loewenschuss, A. *J. Mol. Struct.* **1982**, *78*, 299. (c) Gosavi, R. K.; Greig, G.; Young, P. J.; Strausz, O. P. *J. Chem. Phys.* **1971**, *54*, 983.
- (7) Schwerdtfeger, P.; Dolg, M.; Schwarz, W. H. E.; Bowmaker, G. A.; Boyd, P. D. W. *J. Chem. Phys.* **1989**, *91*, 1762.
- (8) Wang, S. G. Ph.D. Thesis, Siegen University. Verlag Shaker: Aachen, 1994.

- (9) Liao, M. S.; Zhang, Q. E. *Relativistic Density-Functional Study of MX₂ and M₂X₂ Compounds*; Xiamen University: Xiamen, China, 1994.
- (10) Schwerdtfeger, P.; Boyd, P. D. W.; Brienne, S.; McFeaters, J.; Dolg, M.; Liao, M. S.; Schwarz, W. H. E. *Inorg. Chim. Acta* **1993**, *213*, 233.
- (11) Kaupp, M.; von Schnering, H. G. *Inorg. Chem.* **1994**, *33*, 2555, 4179, 4718.

condensed phase. They argued, in contrast e.g. to refs 12 and 13, that the instability of Zn(I) and Cd(I) compounds as compared to the Hg(I) ones could be attributed to the cohesive energies of the metals and to the aggregation or solvation effects of the compounds in the condensed phase, which are modified by relativity. They had carried out calculations on free M_2X_2 and MX_2 ($M = Zn, Cd, Hg$; $X = F, Cl$) and estimated the influence of the condensed phase environment by calculating the dimers $(M_2F_2)_2$ and $(MF_2)_2$, the water adducts $MCl_2 \cdot H_2O$ and $M_2Cl_2 \cdot H_2O$, and the crystals HgF_2 and Hg_2F_2 . We report here on our own, simultaneous, extended investigations on the same general subject,^{4,9} which supply additional and deeper physical understanding of the numerical-empirical findings.

Solid compounds which contain rather localized building blocks can, in most cases, be well treated by the "embedded cluster approximation". I.e. a group of atoms is treated by a molecular quantum mechanical method, while the environment is simulated in an approximate manner. We have shown that such a model is quite suitable for the study of crystalline Hg_2-Cl_2 , Hg_2Br_2 and Hg_2I_2 , while the more pronounced interactions in the fluoride demand a more sophisticated treatment;⁴ see also ref 37. The model correctly describes the effects of the crystalline environment on bond lengths, bond energies, and vibrational frequencies. Accordingly it provides a good model to examine the title compounds in more detail.

Our main interest focuses on the comparison of the relative stability of M_2X_2 vs MX_2 . Our investigation will also comprise the bromine and iodine compounds so that the dependence of the stabilities on electronegativity differences can better be investigated. In addition the MX and MX_2 molecules were calculated. We have determined all known and unknown force constants and frequencies of these species, too.

2. Computational Details

2.1. The Local Density-Functional Method. The AMOL density-functional program¹⁴⁻¹⁶ was used as in our previous work.^{4,5,9,10} The core electrons up to the $(n-1)p$ -shell were kept frozen, and only the valence electrons (ns , np of the halogens; $(n-1)d$, ns of the metals) were permitted to relax. The simple $X\alpha$ potential ($\alpha = 0.7$) was chosen since more sophisticated potentials were shown not to improve the results for this kind of systems.⁴ The bond energy was calculated according to the approach of Ziegler and Rauk.¹⁷ Relativistic corrections to the bond energy were determined in first order.¹⁸

The molecular orbitals were expanded in atomic-centered STO basis sets. For the valence shells, triple ζ basis sets augmented with two p polarization functions on the metals (Zn: $\zeta_{4p} = 2.2$, $\zeta'_{4p} = 1.00$; Cd: $\zeta_{5p} = 2.3$, $\zeta'_{5p} = 1.1$; Hg: $\zeta_{6p} = 2.6$, $\zeta'_{6p} = 1.35$) and double ζ basis sets augmented with one d polarization function on the halogens (F, $\zeta_{3d} = 2.0$; Cl, $\zeta_{3d} = 1.8$; Br, $\zeta_{4d} = 1.9$; I, $\zeta_{5d} = 2.0$) were applied. A single ζ set was added to represent the core wiggles of the valence orbitals. All exponents were taken from ref 16. While the Mulliken populations of the metal $(n-1)d$ -shell hardly vary upon bonding, their shapes do and a flexible triple ζ d -basis is important for the bond energy curve; also the metal np functions are quite important for both electronic structure and bonding, while f -functions are less so.⁴

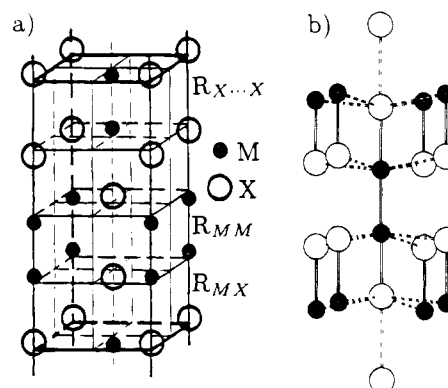


Figure 1. Structure of solid Hg_2X_2 : (a) the unit cell; (b) the local environment of a Hg_2X_2 molecule in the crystal.

Table 1. Lattice Parameters of M_2X_2 (in pm) Used in the Crystal Field Calculations^a

	M_2F_2	M_2Cl_2	M_2Br_2	M_2I_2
$a = b$	367	448	466	492
c ($M = Zn$)	1005	1021	1042	1096
($M = Cd$)	1077	1095	1111	1164
($M = Hg$)	1088	1091	1111	1161
$M-M$ ($M = Zn$)	228	231	232	234
($M = Cd$)	258	261	262	264
($M = Hg$)	251	253	249	269
$M-X$ ($M = Zn$)	184	219	233	253
($M = Cd$)	205	241	254	272
($M = Hg$)	214	243	261	268

^a Experimental data²¹⁻²⁴ for $M = Hg$, slightly corrected; estimated values for $M = Zn$ and Cd .

2.2. Crystal Structure Modeling. In order to investigate the relative stability of the halides in the solid state, their crystal structures are needed. We assumed the crystal structure of Hg_2X_2 for hypothetical solid Zn_2X_2 and Cd_2X_2 , with appropriately scaled lattice constants. A unit cell (tetragonal space group $I4/mmm$, two formula weights of M_2X_2) is shown in Figure 1a. The lattice parameters of the Hg compounds were taken from experimental determinations.¹⁹⁻²⁴ Some of those values are questionable, for instance the Hg-Br distance of 271 pm. Our calculations yield 261 pm, which may still be too large. According to our previous calculations,⁴ the Hg-Hg bond length is nearly the same in different crystalline compounds, and the Hg-X distances are longer by about 0.08 Å than those of the free molecules. Therefore we firstly calculate the free Zn_2X_2 and Cd_2X_2 molecules (see section 3.4) to obtain the bond distances R_{MM}^{free} and R_{MX}^{free} . The lattice constants c were then determined from R_{MM}^{free} and from R_{MX}^{free} elongated as in the case of $M = Hg$ (see Figure 1) according to

$$c = R_{MM}^{free} + 2(R_{MX}^{free} + 0.08 \text{ \AA}) + R[X(1) \cdots X(3)] \quad (3)$$

For $a = b$, we take the same data as in the corresponding Hg_2X_2 structures, since the values of a are determined by the size of the halogen atoms. All lattice parameters are collected in Table 1.

A structural feature of the crystalline Hg_2X_2 compounds (except the fluoride) is that the Hg_2X_2 "molecules" are isolated. Therefore all the other atoms are considered as point charges bearing the formal ionic charge of ± 1 . The corresponding Madelung potential is evaluated^{25,26}

(12) Neisler, R. P.; Pitzer, K. S. *J. Phys. Chem.* **1987**, *91*, 1084.

(13) Pyykkö, P. *Chem. Rev.* **1988**, *85*, 563.

(14) Baerends, E. J.; Ellis, D. E.; Ros, P. *Chem. Phys.* **1973**, *2*, 41; Baerends, E. J.; Ros, P. *Int. J. Quantum Chem. Symp.* **1978**, *12*, 169; te Velde, G.; Baerends, E. J. *J. Comp. Phys.* **1992**, *99*, 84; Snijders, J. G.; Baerends, E. J. *Mol. Phys.* **1978**, *36*, 1789; Snijders, J. G.; Baerends, E. J.; Ros, P. *Mol. Phys.* **1979**, *38*, 1909.

(15) Baerends, E. J., Ed. ADF program package. Free University, Amsterdam, 1989.

(16) Vernooijs, P.; Snijders, J. G.; Baerends, J. E. *Slater type basis functions for the whole periodic system*; Free University: Amsterdam, 1981.

(17) Ziegler, T.; Rauk, A. *Theor. Chim. Acta* **1977**, *46*, 1.

(18) Ziegler, T.; Snijders, J. G.; Baerends, E. J. *J. Chem. Phys.* **1981**, *74*, 1271.

(19) Havighurst, R. J. *J. Am. Chem. Soc.* **1926**, *48*, 2113.

(20) Huggins, M. L.; Magill, P. L. *J. Am. Chem. Soc.* **1927**, *49*, 2357.

(21) Belov, N. V.; Mokeeva, V. I. *Tr. Inst. Krist. Akad. Nauk SSSR* **1949**, *5*, 13.

(22) Grdenic, D.; Djordjevic, C. *J. Chem. Soc.* **1956**, 1316.

(23) Dorm, E. *J. Chem. Soc., Chem. Commun.* **1971**, 466.

(24) Calos, N. J.; Kennard, C. H. L.; Davis, R. L. *Z. Kristallogr.* **1989**, *187*, 305.

(25) Ewald, P. P. *Ann. Phys.* **1921**, *64*, 253.

(26) Almlöf, J.; Wahlgren, U. *Theor. Chim. Acta* **1973**, *28*, 161.

in the region of the M₂X₂ group and then approximated by adjusted charges on a number of crystal lattice points (30–100) in the molecular surrounding. We expect the approximations in the lattice structure to cause only very small errors in the crystal field.

The valence electrons of the M₂X₂ group must not penetrate into the electrostatically attractive core regions of the surrounding cations because of Pauli exclusion. Therefore the Madelung potential has slightly been modified by using a Coulomb cut-off type pseudopotential²⁷

$$V_{\text{eff}}(r) = \text{Max}(V_{\text{Madelung}}(r), C) \quad (4)$$

We have chosen the value of $C = 0.5$ au. The bond energy consists of two parts:

$$E_{\text{bond}}^{\text{total}} = \frac{1}{2}E_{\text{latt}} + E_{\text{bond}}^{\text{internal}} \quad (5)$$

$E_{\text{bond}}^{\text{internal}}$ is the bond energy of the M₂X₂ group, as calculated in the crystal field. E_{latt} is the electrostatic interaction between the M₂X₂ fragment and the lattice

$$E_{\text{latt}} = \int \rho_{\text{M}_2\text{X}_2}(\vec{r}) V_{\text{eff}}(\vec{r}) d\vec{r} + \sum_A^{M_2X_2} Z_A V_{\text{eff}}(R_A) \quad (6)$$

The geometry of the molecule in the crystal field is then optimized by minimizing $E_{\text{bond}}^{\text{total}}$. Since the resulting geometries did not differ from the ones used for the determination of the Madelung potential in eq 3 by more than a few picometers at most, we renounced the iterative readjustment of the Madelung potential.

3. Computational Results

The calculated molecular properties (bond lengths, bond energies, force constants, vibrational frequencies, enthalpies of formation, Mulliken populations) of the free molecules MX, MX₂, M₂X₂ and of the M₂X₂ crystals are collected in Tables 2–8. The PP-MP2 results of Kaupp and von Schnering¹¹ and some available experimental data are also given for comparison.

3.1. Radicals MX (Table 2). Our calculated bond lengths are close to the PP-MP2 values obtained by Kaupp and von Schnering¹¹ for MF and MCl and by Bowmaker and Schwerdtfeger²⁸ for ZnX. Our results on ZnBr and ZnI are longer by 3 and 5 pm than the experimental data. The relativistic effects decrease the M–X bond lengths by about $\Delta^{\text{rel}}R \approx 10 \text{ pm} \times (Z_M^2 + Z_X^2)/c^2$. The calculated bond lengths are well reproduced as sums of effective atomic radii, which are given in the first row of Table 5a.

The calculated frequencies (and force constants) are slightly too low, the average absolute error being about 25 cm⁻¹. The same holds for the values of ref 28. We corroborate the critique by²⁸ of the experimentally based vibrational parameters of ZnBr. Our bond energies are in general slightly overestimated, on the average by 0.3 eV. Some experimental estimates of the bond energies of ZnCl and ZnI seem too large, and concerning those of CdBr and CdI, the experimental upper limits seem to be the better values.

The stability of MX (bond energy, force constant) decreases from F to I, and from Zn to Hg. The latter trend is reinforced for the more polar molecules by relativity (relativistic bond destabilization), i.e. by a relativity–ionicity–cross term. In general, if an electropositive atom (Hg) is stabilized by relativity and is bonded to an electronegative atom (e.g. Hg^{δ+}F^{δ-}),

Table 2. Properties of MX Molecules (M = Zn, Cd, Hg; X = F, Cl, Br, I)^a

		R		
		Zn	Cd	Hg
F	LDF	178 (–1)	201 (–1)	210 (–3)
	PP	179.4, 178.4	201.6	206 (–6.9)
Cl	LDF	215 (–1)	238 (–1)	246 (–4)
	PP	215.2, 216.1	236.9	240.8 (–8.4)
Br	LDF	230 (–1)	252 (–2)	260 (–4)
	PP	234.0		
	Exp	227		
I	LDF	251 (–2)	271 (–3)	280 (–5)
	PP	250.8		
	Exp	246		
		E _{bond}		
		Zn	Cd	Hg
F	LDF	3.48 (–0.15)	3.02 (–0.38)	2.10 (–1.01)
	PP	2.17 ?		
	Exp		3.2	1.8; 1.4 ?
Cl	LDF	2.33 (–0.11)	2.09 (–0.30)	1.34 (–0.82)
	PP	2.13		
	Exp	2.1; 2.6; 3.0 ?	2.15	1.08
Br	LDF	1.89 (–0.11)	1.71 (–0.30)	1.03 (–0.78)
	PP	1.80		
	Exp		(0.9 to) 1.6; 1.5; 2.8 ?	0.75
I	LDF	1.45 (–0.07)	1.34 (–0.25)	0.75 (–0.68)
	PP	1.40		
	Exp	2.0 ?; 1.8 ?; 1.7 ?	(0.4 to) 0.9 ?; 1.4	0.35 ?
		k		
		Zn	Cd	Hg
F	LDF	3.22 (–0.03)	2.48 (–0.06)	1.97 (–0.23)
	PP	3.12		
	Exp	3.42	2.74	2.38
Cl	LDF	1.86 (–0.01)	1.48 (–0.05)	1.22 (–0.14)
	PP	1.84		
	Exp	2.01, 2.07	1.73	1.50
Br	LDF	1.53 (0.00)	1.26 (–0.05)	1.04 (–0.12)
	PP	1.36		
	Exp	2.14 ?, 0.83 ?	1.48	1.18
I	LDF	1.18 (+0.02)	1.03 (0.00)	0.82 (–0.10)
	PP	1.24		
	Exp	1.27	1.13	0.72
		ω		
		Zn	Cd	Hg
F	LDF	609 (–3)	508 (–7)	439 (–25)
	Exp	~628	~535	490.8
Cl	LDF	370 (–1)	305 (–5)	262 (–15)
	Exp	390.5, 387.4, 385	331.0	292.6
Br	LDF	268 (0)	214 (–4)	176 (–10)
	Exp	318 ?, 220 ?, 198 ?	230.5	186.5
I	LDF	217 (+2)	173 (0)	134 (–8)
	Exp	223.4	178.7	125.0

^a Bond length R in pm, bond energy E_{bond} in eV, force constant k in N/cm, vibrational frequency ω in cm⁻¹. LDF = present local density-functional calculations (values in parentheses are the relativistic contributions); PP = pseudopotential MP2 or QCI calculations;^{11,28} Exp = experimental data from refs 1, 2, 6; values with ? seem to be questionable.

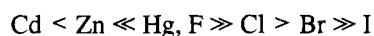
then relativity reduces the bond strength (compare Table 9 of ref 29a). The trend corresponds to the following order

(27) Kutzelnigg, W.; Koch, R. J.; Bingel, W. A. *Chem. Phys. Lett.* **1968**, *2*, 197.

(28) Bowmaker, G. A.; Schwerdtfeger, P. *J. Mol. Struct.* **1990**, *205*, 295.

(29) (a) Schwarz, W. H. E. In *The Concept of the Chemical Bond*; Maksic, Z. B. Ed.; Springer: Berlin, 1990; p 593. (b) Liao, M. S.; Schwarz, W. H. E. *Acta Crystallogr., B* **1994**, *50*, 9.

of elec-tronegativities:



This order agrees with Mulliken electronegativities, though, for the metals, not with Allred–Rochow or Pauling electronegativities. Concerning the relativistic changes of bond lengths, bond energies and force constants, we note that Badger's and Gordy's rules ($\Delta R \sim -\Delta k$ and $\Delta R \sim -\Delta E$) are not even qualitatively fulfilled.

We expect the calculated values for the following species to be of similar accuracies as those estimated above ($\delta R \sim 3$ pm, $\delta\omega \sim 25$ cm⁻¹, $\delta E \sim 0.3$ eV).

3.2. MX₂ Molecules (Table 3). The trends of the bond lengths of MX₂ and MX are similar. The bond lengths of MX₂ are, however, somewhat shorter than those of MX, especially for the heavier M and X. The corresponding effective atomic radii in MX₂ are given in Table 5a. The relativistic bond length contractions are more pronounced in MX₂: $\Delta^{\text{rel}}R \approx 20$ pm $\times (Z_M^2 + Z_X^2)/c^2$.

The energies and force constants of the M–X bonds in MX₂ are larger than in MX. $\delta E = E(\text{XM–X}) - E(\text{M–X})$ is of the order of 1 eV. Relativity reduces the MX₂ bond energies, but this effect does no longer vary so strongly with the electronegativity difference than in MX. In contrast to MX, the force constants are relativistically increased, but still not proportional to $-\Delta^{\text{rel}}R$, as would have been expected according to Badger's rule. Concerning the accuracies, we note that the LDF energies are somewhat large while the PP energies¹¹ are somewhat low. Both trends are not unusual.

3.3. M₂X₂ Molecules (Table 4). Our results on the fluorides and chlorides are again in accord with those of Kaupp and von Schnering.¹¹ The effective radii of the metals for the central M–M bonds steadily increase by 6 pm upon replacing the electron-withdrawing fluorine by Cl, Br, and I, i.e. by 3 pm per electronegativity unit. Cd and Hg have very similar radii (Table 5a), as in the case of the metallic state. The quite large relativistic bond contraction of about 63 pm $\times (Z_M^2/c^2)$, and also the lanthanoid contraction⁴ are both responsible for the fact that Hg is hardly bigger than Cd (compare the same phenomenon for Ag and Au^{29b}).

The effective radii for the M–X bonds are also given in Table 5a. The effective radii of the halogens are nearly equal in the three series MX₂, M₂X₂, MX, and similar to the values given in standard tables, while the radii of the metals are much more sensitive to the environment (see Table 5b). This is not an artifact due to choosing a halogen radius as reference value. The M–X bond lengths vary in the order MX₂ < M₂X₂ < MX (see Table 5c). The relativistic bond contractions of the M–X bonds in M₂X₂ are comparable to those in MX₂.

The M₂X₂ molecular potential energy hypersurfaces have (local) minima of linear *D_{∞h}* geometry. The 7 vibrational species are of σ_g (ω_1 , M–M stretch), σ_g (ω_2 , M–X symmetric stretch), σ_u (ω_4 , M–X asymmetric stretch), π_g (ω_5 , bend), and π_u type (ω_3 , bend). Concerning the bond stretching modes (see Scheme 1) the energy is given in the harmonic approximation by

$$2E = k_{\text{MM}}\Delta R_{\text{MM}}^2 + k_{\text{MX}}(\Delta R_{\text{MX}_1}^2 + \Delta R_{\text{MX}_2}^2) + 2k_{12}(\Delta R_{\text{MX}_1} + \Delta R_{\text{MX}_2})\Delta R_{\text{MM}} \quad (7)$$

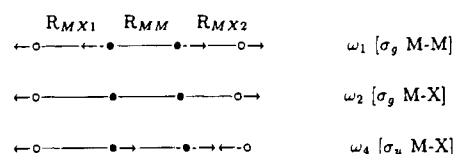
Both diagonal harmonic force constants increase from the iodides to the fluorides and vary in the order Hg > Zn > Cd (nonrelativistic: Zn > Cd \approx Hg) for k_{MM} , and in the order Zn > Hg > Cd (nonrelativistic: Zn \gg Cd > Hg) for k_{MX} . The

Table 3. Properties of MX₂ Molecules^a

		R		
		Zn	Cd	Hg
F	LDF	172 (–1)	193 (–3)	197 (–7)
	PP	174.1	195.9	196.5 (–11.4)
	Exp	181 ? , 174.2		
Cl	LDF	207 (–1)	228 (–3)	231 (–9)
	PP	208.9	229.2	229.3 (–12.8)
	Exp	206.2	224	227 to 234, 225.2
Br	LDF	221 (–2)	241 (–4)	245 (–9)
	PP			242.1 (–12.5)
	Exp		235	241
I	LDF	241 (–2)	260 (–4)	263 (–10)
	PP			262.1 (–12.2)
	Exp	242	260; 258	259
		E _{bond}		
		Zn	Cd	Hg
F	LDF	4.51 (–0.09)	3.93 (–0.25)	3.25 (–0.64)
	PP	3.88	3.30	2.49 (–0.81)
	Exp			2.66
Cl	LDF	3.35 (–0.07)	2.97 (–0.20)	2.42 (–0.52)
	PP	3.01	2.644	2.00 (–0.68)
	Exp	3.31		2.34
Br	LDF	2.86 (–0.08)	2.57 (–0.20)	2.04 (–0.53)
	PP			1.86 (–0.85)
	Exp			1.92
I	LDF	2.37 (–0.06)	2.17 (–0.17)	1.71 (–0.46)
	PP			1.33 (–0.95)
	Exp			1.51
		k		
		Zn	Cd	Hg
F	LDF	4.34 (+0.09)	3.35 (+0.12)	3.35 (+0.40)
Cl	LDF	2.75 (+0.06)	2.24 (+0.12)	2.29 (+0.34)
Br	LDF	2.28 (+0.03)	1.93 (+0.10)	1.98 (+0.27)
I	LDF	1.85 (+0.04)	1.60 (+0.07)	1.63 (+0.21)
		ω_{σ_g}		
		Zn	Cd	Hg
F	LDF	622 (+6)	547 (+10)	547 (+34)
	PP			577
	Exp	596	555	568
Cl	LDF	362 (+3)	327 (+9)	331 (+26)
	PP			346
	Exp	295		358
Br	LDF	220 (+2)	202 (+5)	205 (+15)
	PP			215
	Exp	225		225
I	LDF	161 (+2)	150 (+4)	148 (+10)
	PP			154
	Exp			164

^a See footnote of Table 2. E_{bond} and k correspond to a single M–X bond. The experimental bond energies are estimated from the standard enthalpies of the molecules in the gas phase (see Table 6). For experimental data see also refs 39–41.

Scheme 1



large relativistic increase of the force constants of the mercury compounds is responsible for the unusual orders. The coupling force constants k_{12} are only on the order of 0.01 N/cm and are

not listed in Table 4. The MM-force constants decrease slightly in the order of decreasing electronegativity of the halogens.

The dissociation energies of the XM–MX bonds vary according to Zn > Hg ≫ Cd for the fluorides and according to Zn ≫ Hg > Cd for the iodides. (At the nonrelativistic level, the M–M bond energies still vary in the “normal” order Zn > Cd > Hg.) The bond energies increase with increasing electronegativity of the ligand (compare with ref 10), i.e. from the iodides to the fluorides by 0.35 eV for Cd, by 0.45 eV for Zn, and by 0.6 eV for Hg. The comparatively strong Hg–Hg bonds (2.2–2.8 eV) are relativistically *stabilized*, as already noted in the literature,^{4,10,11} in contrast to the M–X. The relativistic stabilizations depend in a nonadditive manner on both $(Z/c)^2$ and the MX bond polarities.

3.4. M₂X₂ in the Solid State. When the molecules are imbedded in the crystal, the M–X bonds expand (as to be expected for the increased coordination number in the solid) by about 8–10 pm, while the M–M bonds are hardly influenced. Concerning the crystallographic experiments, the more recent neutron diffraction result²⁴ of 260 pm for ClHg–HgCl as well as the X-ray values of 256–258 pm for Cd–Cd in Cd₂(AlCl₄)₂^{30–32} agree with the calculated ones. Most other experimental results on Hg(I) halides^{19–22,33} seem questionable, especially concerning the pretended Hg–Hg bonds length increase from the fluoride to the iodide by more than 20 pm, the respectively small increase of Hg–X bond lengths from X = F to I by only ~40 pm (instead of ~70 pm, corresponding to standard halogen radii) and the diverse “theoretical explanations” developed for these “phenomena” (for details see ref 4). We corroborate the approximate constancy of the Hg–Hg distances as found by Dorm,²³ whereas his absolute values seem too small by about 10 pm.

The crystal field modifies (i.e. increases) the M–M force constants of the Hg-species, and the M–M bond energies of all compounds, whereas the M–X force constants are reduced. The significant crystal field stabilization of the M–M bond of M₂X₂ can be described by increments $\Delta M + \Delta X$ with $\Delta Zn = 1.1$ eV, $\Delta Cd = 1.6$ eV, $\Delta Hg = 1.5$ eV, $\Delta F = 1.0$ eV, $\Delta Cl = 0.6$ eV, $\Delta Br = 0.5$ eV, and $\Delta I = 0$ as reference value. Due to the relatively small increment for Zn, the order of the M–M bond energies is changed from Zn > Hg > Cd (see section 3.3) to Hg > Cd ≫ Zn in the crystal. This order had also been deduced from the Raman spectra.¹ It is to be noted that the special stability of the Hg–Hg bond occurs in the solids, although there exists a relativity–crystal field–cross term which destabilizes the Hg–Hg bond by ~0.55 eV, while the Cd–Cd and Zn–Zn bonds are destabilized by only ~0.25 and ~0.1 eV, respectively.

Within the rather wide ranges of experimental^{32–34} and theoretical (± 0.3 eV) accuracies, there is agreement between measured and calculated bond energies. The few experimental frequencies of the M–M vibrations are only 5–9 cm⁻¹ bigger than the calculated ones, those of the M–X vibrations are 13–34 cm⁻¹ smaller. The calculated M–X σ_g/σ_u splittings are mainly due to mass-coupling; thus, they are negligible for Hg₂F₂ and largest (about 100 cm⁻¹) for Zn₂I₂. Because of the mass coupling, Badger’s rule as applied in ref 31 will not yield reliable estimates of the Hg–Hg bond lengths.

With the help of the experimental vaporization enthalpies of fluid bromine (0.31 eV), solid iodine (0.63 eV) and the metals (contrary to Kaupp,¹¹ we include the melting heats of Zn and Cd, i.e. we use $\Delta H(Zn) = 1.36$ eV, $\Delta H(Cd) = 1.12$ eV, and $\Delta H(Hg) = 0.64$ eV), of the calculated dissociation energies of the halogen molecules (experimental values in parentheses: $D(Cl_2) = 2.91$ (2.51) eV, $D(Br_2) = 2.38$ (1.99) eV, $D(I_2) = 2.08$ (1.56) eV), the energies in Tables 2–4, and the lattice energies according to eq 6, we can determine the energies of formation of solid M₂X₂. By using the calculated $D(X_2)$ -values, which are 0.4 eV too large, we expect that the errors in the calculated values for M₂X₂ partially cancel. They are presented in Table 6. According to our previous experience⁴ on solid Hg₂F₂, the crystal field model is not so adequate because of the close approach and overlap of the atoms of adjacent molecules (see also ref 37). Therefore the fluorides are not included in Table 6. For comparison we include the standard enthalpies of formation of the Hg(I) compounds from experimental thermodynamic data.^{35,36} The difference between standard enthalpies and zero point energies is only of the order of several 0.01 eV and is neglected here. The reasonable agreement of the theoretical formation energies and the experimental standard formation enthalpies gives some confidence in the calculated values. Relativity destabilizes the M(I) compounds by about 5.5 eV $\times (Z_M/c)^2$, i.e. Zn₂X₂ by ~0.3 eV, Cd₂X₂ by ~0.7 eV and Hg₂X₂ by ~1.8 eV.

Comparing with the experimental standard enthalpies of formation of MX₂^{35,36} in Table 6 we see that M₂X₂ are unstable with respect to solid state disproportionation by about 1 eV in the case of Zn₂X₂ and by about 0.7 eV in the case of Cd₂X₂, but the Hg₂X₂ are stable by up to several tenths of an electron-volt. For all three metals, the monovalent state is (relatively) stabilized by the more electronegative ligands.

3.5. Charge Distributions and Hybridization (Table 7). The atomic Mulliken charges on the halogens are very similar in the different molecules (MX, MX₂, M₂X₂); therefore, only the average values are given in Table 7. There are no pronounced differences with respect to the three metals, while the variation with respect to the halogens corresponds to their standard electronegativities: F ≫ Cl > Br ≫ I. The differences of the three heavy halogens are mainly attributable to relativistic effects. It is well-known^{13,28} that the $np_{3/2}$ valence levels of the halogens are significantly destabilized by spin–orbit coupling and by relativistic nuclear shielding. It is noteworthy that the Mulliken charges of M₂X₂ increase quite a bit in the crystal field. This increase is more pronounced for weakly polar molecules, i.e. it is only 0.2 e for the strongly polar fluorides, and about 0.4 e for the less polar iodides. The dipole moments of the MX molecules correspond to the usual order of halogen electronegativities and to metallic electronegativities of the order Cd < Zn ≈ Hg.

The $(n - 1)d$ shell on the M is occupied, in general by 9.9–10.0 electrons; i.e., the d-shell does not directly participate in covalent bonding. On the other hand, there is significant metal np population corresponding to hybridizations in the range from $sp^{0.1}$ to $sp^{0.7}$. The $M(ns/np)$ mixing due to bonding increases

(30) Faggiani, R.; Gillespie, R. J.; Vekris, J. E. *J. Chem. Soc., Chem. Commun.* **1986**, 517.

(31) Staffel, Th.; Meyer, G. Z. *Anorg. Allg. Chem.* **1987**, *548*, 45.

(32) Corbett, J. D. *Inorg. Chem.* **1962**, *1*, 700.

(33) Stammreich, H.; Teixeira Sans, T. *J. Mol. Struct.* **1967**, *1*, 55.

(34) Stull, D. R.; Sinke, G. C. *Thermodynamic Properties of the Elements*, Advances in Chemistry 18; American Chemical Society: Washington, DC, 1956.

(35) Wagman, D. D.; Evans, W. H.; Parker, V. B.; Halow, I.; Bailey, S. M.; Schumm, R. H. *Selected Values of Chemical Thermodynamic Properties*; NBS Technical Notes 270-3/4; National Bureau of Standards: (U.S.), Washington, DC, 1968/9. Stull, D. R.; Prophet, H. *JANAF Thermochemical Tables*; NSRDS-NBS 37, 2nd ed.; US-DOC/NBS: Washington, DC, 1971.

(36) Barin, I.; Knacke, O. *Thermochemical Properties of Inorganic Substances*; Springer: Berlin, and Verlag Stahleisen: Düsseldorf, Germany, 1973.

(37) Pascual, J. L.; Seijo, L.; Barandiaran, Z. *J. Chem. Phys.* **1993**, *98*, 9715.

Table 4 (Continued)

		$\omega_4(M-X)$					$\omega_4(M-X)$		
F	LDF	664 (-7)	540 (-17)	583 (+82)	Br	LDF	303 (-8)	245 (+6)	223 (+16)
Cl	LDF	415 (-7)	349 (+4)	335 (+4)	LDF-CF	252	218 (+8)	195 (+14)	
	LDF-CF	345	311 (+17)	295 (+31)		Exp			180
	Exp			261		I	LDF	252 (-2)	204 (+8)
					LDF-CF	217	175 (+6)	169 (+14)	
					Exp			138	

^a See footnote of Table 2. ^b CF = molecule in crystal field. Exp(c) = molecule in the crystal; for references for experimental data, see refs 1 and 4, values in parentheses are questionable. E_{MM} refers to reaction 1, both molecules being optimized. ^b Extended basis-QCI-SD(T) calculation of ref 11. ^c References 30-32. ^d Reference 24.

Table 5

(a) Effective Atomic Radii, in pm							
system	Zn	Cd	Hg	F	Cl	Br	I
metal	134	149	150				
XM-MX	116	131	132				
M-X	117	139	147	62	99 ^a	113	133
XM ₂ -X	112	133	139	64	99 ^a	113	132
XM-X	108	128	132	65	99 ^a	113	132
(b) Change of Effective Radii from Zn to Cd and from Cd to Hg, in pm							
system	R(Cd)-R(Zn)		R(Hg)-R(Cd)				
metallic solid	15		1				
XM-MX	15		0				
XM-X	20		3				
XMM-X	21		5				
M-X	22		8				
std ionic radii	19		18				
(c) Change of M-X Bond Lengths in the Sequence MX ₂ -M ₂ X ₂ -MX							
metal	R(XMM-X) - R(XM-X)		R(M-X) - R(XMM-X)				
Zn	4		4				
Cd	5		6				
Hg	7		8				

^a Cl radius = 99 pm chosen as the reference value.

Table 6. Calculated Energies of Formation (I) of Solid M₂X₂, with Relativistic Contributions in Parentheses (Exp = Experimental Standard Enthalpies of Formation), Experimental Standard Enthalpies (II) of Formation of Solid MX₂, and Difference (Δ) between I and II^a

		Zn	Cd	Hg
Cl	I	-3.38 (+0.26)	-3.44 (+0.69)	-3.00 (+1.82)
	E_{latt}	-0.15	-0.27	-0.31
	II	-4.32	-4.06	-2.39
Δ	0.94	0.62	-0.61	
Br	I	-2.50 (+0.32)	-2.64 (+0.73)	-2.28 (+1.83)
	E_{latt}	-0.11	-0.18	-0.21
	II	-3.40	-3.27	-1.76
Δ	0.90	0.63	-0.52	
I	I	-0.99 (+0.42)	-1.33 (+0.78)	-1.11 (+1.77)
	E_{latt}	-0.01	-0.06	-0.08
	II	-2.17	-2.12	-1.09
Δ	1.18	0.79	-0.02	

^a All energies in eV.

in the order F < Cl \approx Br < I as anticipated by Lewis,³⁸ in the order Zn > Cd > Hg, and in the order MX < M₂X₂ (solid) < M₂X₂ \approx MX₂. At the nonrelativistic level of approximation, there is no change of M(ns/np) hybridization for different halogen ligands in a given molecular series (Hg sp^{0.43} for HgX₂, Hg sp^{0.3} for Hg₂X₂, Hg sp^{0.24} for HgX, and only Hg sp^{0.12} for

Table 7. Average Mulliken Charges \bar{q} ($X^{q-} - M^{q+}$; $X^{q-} - M^{2q+} - X^{q-}$; $X^{q-} - M^{q+} - M^{q+} - X^{q-}$) and q_s of M₂X₂, X₂ in the Solid, Dipole Moments μ of MX (in D), and M_{ns}/M_{np} Populations in MX, MX₂, M₂X₂, and M₂X₂ (s = Solid) with Relativistic Contributions in Parentheses

		Zn	Cd	Hg	
F	\bar{q}	0.59 (-0.02)	0.60 (-0.03)	0.54 (-0.08)	
	q_s			0.77	
	μ	2.5 (-0.1)	3.2 (-0.1)	3.0 (-0.5)	
	MF	1.13 // 0.30	1.20 // 0.25	1.42 // 0.14 (+0.26 // -0.11)	
	MF ₂	0.57 // 0.32	0.64 // 0.26	0.91 // 0.19 (+0.31 // -0.05)	
M ₂ F ₂	M ₂ F ₂	1.06 // 0.37	1.08 // 0.36	1.10 // 0.40 (+0.01 // +0.07)	
	M ₂ F ₂ (s)			1.03 // 0.24	
	Cl	\bar{q}	0.39 (-0.02)	0.42 (-0.04)	0.39 (-0.08)
		q_s	0.69	0.75 (-0.02)	0.74 (-0.04)
μ		2.4 (-0.1)	3.2 (-0.2)	2.7 (-0.9)	
MCl		1.23 // 0.37	1.27 // 0.30	1.48 // 0.19 (+0.25 // -0.11)	
MCl ₂		0.77 // 0.48	0.80 // 0.40	0.98 // 0.31 (+0.21 // -0.04)	
M ₂ Cl ₂	M ₂ Cl ₂	1.13 // 0.48	1.14 // 0.44	1.13 // 0.46 (-0.04 // +0.10)	
	M ₂ Cl ₂ (s)	1.06 // 0.25	1.04 // 0.21	1.04 // 0.25 (-0.03 // +0.15)	
	Br	\bar{q}	0.32 (-0.06)	0.36 (-0.07)	0.32 (-0.11)
		q_s	0.66	0.72 (-0.05)	0.70 (-0.08)
μ		2.3 (-0.2)	3.1 (-0.3)	2.6 (-1.1)	
MBr		1.29 // 0.37	1.32 // 0.30	1.52 // 0.19 (+0.26 // -0.11)	
MBr ₂		0.85 // 0.53	0.88 // 0.44	1.04 // 0.35 (+0.21 // -0.01)	
M ₂ Br ₂	M ₂ Br ₂	1.15 // 0.53	1.16 // 0.48	1.15 // 0.51 (-0.05 // +0.16)	
	M ₂ Br ₂ (s)	1.07 // 0.27	1.06 // 0.22	1.05 // 0.27 (-0.05 // +0.15)	
	I	\bar{q}	0.16 (-0.14)	0.21 (-0.14)	0.17 (-0.18)
		q_s	0.57	0.62 (-0.14)	0.57 (-0.20)
μ		1.9 (-0.3)	2.6 (-0.5)	2.1 (-1.3)	
MI		1.36 // 0.42	1.38 // 0.35	1.58 // 0.23 (+0.27 // -0.08)	
MI ₂		0.99 // 0.70	0.99 // 0.57	1.13 // 0.48 (+0.20 // +0.08)	
M ₂ I ₂	M ₂ I ₂	1.12 // 0.75	1.14 // 0.66	1.14 // 0.67 (-0.09 // +0.29)	
	M ₂ I ₂ (s)	1.04 // 0.39	1.03 // 0.35	1.04 // 0.40 (-0.07 // +0.28)	

Table 8. Density Functional Calculated Heats of Reaction 2 in kJ/mol^c for M₂X₂(g) \rightarrow MX₂(g) + M(g/s)^a

	M = Zn	M = Cd	M = Hg
M ₂ F ₂	84 (-3) // -47	68 (-7) // -44	51 (-19) // -10
	[81 to 37 ^b // -79 ^b]	[88 to 29 ^b // -71 ^b]	[54 to 7 ^b (-40) // -54]
M ₂ Cl ₂	68 (-3) // -63	58 (-8) // -54	38 (-24) // -23
	[72 to 30 ^b // -85 ^b]	[74 to 22 ^b // -78 ^b]	[38 to -6 ^b (-41) // -67]
M ₂ Br ₂	67 (-4) // -64	54 (-9) // -58	36 (-22) // -25
M ₂ I ₂	61 (-4) // -70	49 (-10) // -63	30 (-25) // -31

^a g = gas; s = solid. Values in parentheses are the relativistic contributions. ^b Values in brackets are extended basis set MP2 and QCI-SD(T) calculation of ref 11. ^c 1 eV = 96.5 kJ/mol.

solid Hg₂X₂). This is another example of nonadditive relativistic cross term effects. The remarkable reduction of s-p mixing upon embedding M₂X₂ in the crystal at the relativistic and nonrelativistic levels of theory may be attributed to the higher symmetry of the metal atoms' surrounding (see Figure 1) as compared to the free molecule.

(38) Lewis, J. *Pure Appl. Chem.* **1965**, *10*, 11.

(39) Givan, A.; Loewenschuss, A. *J. Chem. Phys.* **1976**, *64*, 1967; **1980**, *72*, 3809.

(40) Hargittai, M. *Coord. Chem. Rev.* **1988**, *94*, 78.

Table 9. Atomic Increments Δ (in kJ/mol) To Estimate Reaction Energies by $\Delta E \approx \Delta_M + \Delta_X^a$

row	reaction		M			X			
			Zn	Cd	Hg	F	Cl	Br	I
1	$M_2X_2(g) \rightarrow MX_2(g) + M(g)$	$\Delta^{(2)} =$	61 (21)	50 (13)	31 (-12)	21 (17)	8 (-8-)	5	-0-
2	$MX_2(g) + M(g) \rightarrow 2MX(g)$	$\Delta^{(a)} =$	177	155	190	25	18	9	-0-
3	$M_2X_2(g) \rightarrow 2MX(g)$	$\Delta^{(-b)} =$	238 (226)	204 (198)	220 (236)	46 (39)	27 (27)	15	-0-
4	$M_2X_2(g) \rightarrow MX_2(g) + M(s,l)$	$\Delta^{(2')} =$	-70	-63	-31	21	8	5	-0-
5	$M_2X_2(s) \rightarrow MX_2(s) + M(s,l)$	$\Delta^{(2s)} =$	-12 ₀	-9 ₀	+2 ₀	5 ₀	3 ₀	3 ₀	-0-
6	$M_2X_2(s \rightarrow g) + MX_2(g \rightarrow s)$	$\Delta^{tr} =$	-3 ₀	-1 ₀	+7 ₀	0	-0-	0	-2 ₀
7	$M_2X_2(s \rightarrow g)$	$\Delta^{sub} =$	+8 ₀	+10 ₀	+12 ₀	10 ₀	4 ₀	2 ₀	-0-

^a Values between hyphens are the reference values for a given row. Values in parentheses are the best ones of ref 11. The values of rows 5–7 are the least accurate ones. Subscripted digits are completely uncertain.

4. Theoretical Conclusions and Summary

We have performed relativistically corrected local density functional calculations on the free molecules MX, MX₂, and M₂X₂ and on M₂X₂ in the crystal, for X = halogen and M = group 12 atoms. The main defect of our approach is the crystal field embedding. From the explicit calculation of larger Hg–X clusters,⁴ we know that the assumption of purely electrostatic interactions in the crystal breaks down for the fluorides. In the case of the chlorides, bromides and iodides, the direct orbital interactions between adjacent molecules in the solid changes the interatomic distances still by a few pm.

The theoretical estimates of experimentally unknown or inaccurately known molecular parameters such as geometries, bond energies, thermodynamic stabilities, stretching force constants and vibrational frequencies are given in Tables 2, 3, 4, and 7 (dipole moments of MX). Approximate values for the energies of the reaction M₂X₂(s) → MX₂ + M(s/l) are given by Δ in Table 6, and for the reaction M₂X₂(g) → MX₂(g) + M(g) or M(s/l) in Table 8. These theoretical estimates are the most complete ones available at present. They are probably as reliable as the PP-MP2 and PP-QCI results obtained for some of the species by Kaupp and von Schnering.¹¹ The expected inaccuracies of the predictions are a few pm for the bond lengths, a few 0.1 eV or a few 10 kJ/mol for the energies, a few 10 cm⁻¹ for the frequencies, and a few 0.1 D for the dipole moments, except for the solid fluorides. As mentioned above, the very strong intermolecular interactions especially in the fluorides are not appropriately accounted for in the crystal field calculations. Also the experimental heats of formation of MF₂, which are used for the estimates in Table 9, are far from being certain due to decomposition near the vaporization temperatures.

Calculations have also been carried out at the nonrelativistic level of approximation to assess the relativistic contributions. Strong relativity-ionicity cross-effects are found. Many trends are at best understood in terms of the electronegativity order Cd < Zn << Hg. The metals are significantly s–p hybridized. However the p population decreases with increasing ionicity. While the bond polarity increases strongly from the molecular iodides to the molecular fluorides, the polarities are less different, but much higher in the solid compounds.

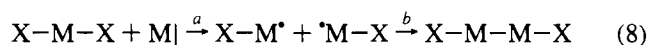
4.1. Stability of M₂X₂ in the Gas Phase. We have a complete data set for the three group 12 and the four group 17 atoms. This is sufficient material to explain or rationalize and understand, with the help of common theoretical model concepts, the trends of the empirical findings from our computer experiments, which were described in the previous sections. According to Tables 4 and 8, all monovalent species M₂X₂ are *stable in the gas phase* against any decomposition into gas phase

products. The endothermicity of reaction (2) can be described very simply by $\Delta E(2) \approx \Delta_M^{(2)} + \Delta_X^{(2)}$, where the increments $\Delta^{(2)}$ are given in the first line of Table 9. $\Delta_I^{(2)} = 0$ is used as the reference value. We see that the Zn(I) and the F compounds are the most stable ones. By the way, there exists experimental evidence¹ that Zn₂X₂ is formed from Zn and ZnX₂ at higher temperatures around 600 K in the gas phase. Relativity contributes by $\Delta^{rel}E(2) \approx -(63Z_M^2 + 15Z_X^2)/c^2$ kJ/mol to the trend of reducing the stability of M₂X₂ from Zn₂F₂ to Hg₂I₂.

We note that our LDF values are more positive than the PP-CI values from ref 11, where $\Delta_{Hg}^{(2)}$ is even negative. Since X α bond energies are usually too big while CI energies are usually too small, the true values for the increments may be in between. Then the statement on the stability of M₂X₂ will still hold, although the heavier Hg₂X₂ species may have very small decomposition energies. Then, at low pressure, the entropy effect may favor disproportionation of Hg₂I₂, Hg₂Br₂, and Hg₂Cl₂.

Now we want to understand *why* the M₂X₂ molecules are stable in the gas phase and *how* the above-mentioned trends come about.

First, we compare the stability of X–M–X with X–M + M–X. From the data of Tables 2 and 3, we find that the endothermicity of the first step of the hypothetical reaction

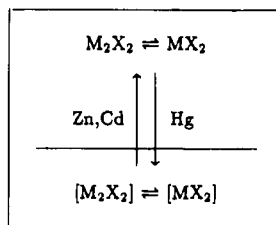


can be approximated by $\Delta E(8a) \approx \Delta_M^{(a)} + \Delta_X^{(a)}$ (plus a small ionicity-relativity cross-term, which increases $\Delta E(8a)$). The increments $\Delta^{(a)}$ are given in the second row of Table 9. The trends can be explained as follows: In order to form an X–M bond, the closed M(*ns*²) shell must be broken up and promoted. This must occur once for MX₂, but twice for 2MX. Therefore the $\Delta^{(a)}$ values are large and positive. The order of the $\Delta_M^{(a)}$ values corresponds to the ones of the s² ionization potentials or the s² → sp excitation energies of M, which vary in the order Cd < Zn < Hg. The large values for Hg are due to its large relativistic (and lanthanide⁴) stabilization of the *ns*-shell. Concerning the dependence of $\Delta E(8a)$ on the halogen, we note that the population of the M(*ns*) shell decreases, i.e. the unpaired electron number on M increases, with increasing electronegativity of X (see Table 7).

Second, we analyze the second step of reaction 8, i.e. eq 1. The increments of $\Delta E(1) \approx \Delta_M^{(-b)} + \Delta_X^{(-b)}$, obtained from Table 4 are given in row 3 of Table 9. For the more electronegative halogen, since there is more single-electron character on the metal atom of MX, more energy is released upon the formation of the XM–MX covalent bond. This explains the dependence on the halogen. The comparatively large value of Δ_{Hg} is again due to the relativistic stabilization and contraction of the Hg(*ns*) shell.

(41) Kashiwabara, K.; Konaka, S.; Kimura, M. *Bull. Chem. Soc. Jpn.* **1973**, *46*, 410.

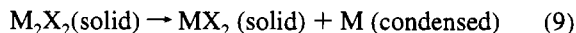
Scheme 2



The increments for the reaction of interest, eq 2, are $\Delta^{(2)} \approx \Delta^{(-b)} - \Delta^{(a)}$. The M₂X₂ molecules are stable, because the $\Delta^{(-b)}$ are larger than the $\Delta^{(a)}$. This is so because, as usual, covalent bond formation ($M^{\bullet} + \bullet M \rightarrow M-M$) in step 8b releases more energy than is needed for the ns^2 -promotion in step 8a. M₂X₂ is stable, because it has one bond more than MX₂ + M. This situation becomes more pronounced, the more single-electron character on the M in MX due to more electropositive metals and more electronegative ligands (compare also [10]). This qualitatively explains the signs and the trends of the Δ_M and Δ_X increments for the gas phase disproportionation in row 1 of Table 9.

When the metal condenses, the stability and the trend with respect to the metals is reversed. The number of M–X and M–M bonds in the reaction of row 4 in Table 9 is not changed any longer. But the M–M bonds in the metals, especially in Cd and Zn, are stronger than the localized ones in M₂X₂ owing to their delocalized character. Thus the Hg(I) and the F compounds are the least unstable ones.

4.2. Stability of M₂X₂ in the Solid Phase. Let us look at the M₂X₂ ⇌ MX₂ equilibria in the gas and solid phases. Hg(I) is more stable in the solid than in the gas phase, whereas the opposite holds for the Cd(I) and more so for the Zn(I) compounds. The reaction energy increments Δ^r for the transfer of the metal between the phases (see Scheme 2) are given in row 6 of Table 9. They may also be interpreted as contributions to the sublimation energy differences between M₂X₂ and MX₂. Increments for the sublimation energies of solid M₂X₂, derived from our calculations, are given in the last row of Table 9. According to row 6, it is easier by about 30 and 10 kJ/mol to sublime Zn₂X₂ or Cd₂X₂ than ZnX₂ or CdX₂, because of the large lattice energies of MX₂¹ with highly charged M^{2q+} ions (Table 7). This explains why the Zn(I) and Cd(I) compounds are even more unstable in the solid than in the gas phase with respect to the disproportionation



On the other hand, it is much easier to sublime HgX₂ than Hg₂X₂. For example, the sublimation energy of HgF₂^{1,35} is only ~ 130 kJ/mol, while that of Hg₂X₂ is ~ 210 kJ/mol (our estimate; Kaupp¹¹ only obtains ~ 170 kJ/mol).

It is remarkable that the energies of the reaction in the row 6 of Table 9 mainly depend on the metal, and much less on the ligand. Ionicity stabilizes the monovalent state,¹⁰ and it stabilizes M₂X₂ in the crystal. However, since the less ionic M–X bonds increase their ionicity upon solidification more than the more ionic ones (Table 7), the ionicity contributions to Δ^r partially cancel.

There are a set of questions untackled so far. Are the presumed crystal structures of M₂X₂ locally stable, or would

Table 10. Relativistic Corrections and Coefficients of Fractional Relativistic Change $\Delta^{\text{rel}} A/A \approx \text{const} (Z_M^2/c^2)$

		const
<i>R_e</i>	large contraction for M–M in M ₂ X ₂ (g, s)	–0.25
	medium contraction for M–X in MX ₂ , M ₂ X ₂ (g, s)	–0.1
	small contraction for M–X in MX	–0.05
<i>D_e</i>	medium stabilization for M–M in M ₂ X ₂ (g)	<i>a</i>
	large destabilization for M–X in MX	(–2)
	medium destabilization for M–X in MX ₂	–0.6
	medium destabilization for M–M in M ₂ X ₂ (s)	<i>a</i>
<i>k</i>	large increase for M–M in M ₂ X ₂ (g, s)	+1.2
	small increase for M–X in MX ₂	+0.4
	small decrease for M–X in MX	–0.4
	variable changes for M–X in M ₂ X ₂ (g,s)	<i>a</i>

^a Due to large relativity–ionicity cross terms of different signs, even no approximate proportionality constant can be given.

they distort spontaneously? What is the height of a possible activation barrier of reaction 9? Are the first disproportionation products created in high-energy phases? Accordingly, the question whether Cd₂X₂ or Zn₂X₂ may exist as metastable phases is still open.

4.3. Relativistic Effects. Ample evidence has been found that relativistic corrections to bond energies, force constants, etc. are not simply additive. The relativistic mass-velocity effect^{29a} contracts the M–X and M–M bonds and increases (though not always) the force constants. The bond energies show a more complex behavior (see Table 10). Obviously, Badger's and Gordy's rules cannot be applied to relativistic changes.

Covalent bond formation of M requires singly occupied atomic orbitals, which are harder to achieve for relativistically stabilized Ms² shells. This causes a relativistic destabilization of the M–X bonds, and the destabilization increases for increasing bond polarity, i.e. decreasing *Mns*-population. On the other hand, bond polarity increases the bond strengths, as usual, at the nonrelativistic level. The dependence of the relativistic bond energy changes on the polarities is especially pronounced for the M–M bonds, which are relativistically stabilized in the less polar M₂X₂ molecules, but destabilized in the more polar solids.

MX₂ with one M^{2q+} and M₂X₂ with two M^{q+} are similarly destabilized by relativity in the gas phase (strictly speaking, the destabilization is slightly larger for M₂X₂, e.g. a little more than 20 kJ/mol for Hg₂X₂). But in the more ionic solids, the above-mentioned ionicity–relativity cross term dominates and destabilizes solid MX₂ drastically in comparison to M₂X₂ (by nearly 100 kJ/mol for the Hg compounds). This explains, why Hg(I) is stable in solid Hg₂X₂ in contrast to Zn(I) and Cd(I).

Acknowledgment. We acknowledge comments by Dr. R. Dronskowski, and by a reviewer. This work has financially been supported by the National Natural Science Foundation of China (R.P. No. 040-00387), by the China Postdoctoral Science Foundation, by the Deutsche Forschungsgemeinschaft, and by the Fonds der Chemischen Industrie. We are grateful to Prof. E. J. Baerends and his group for supplying us with their density functional code and for their support in applying it. We thank Ing. D. H. Duong for his help in composing the manuscript.

IC950537R